



# Direct observation of ferroelectric domains and phases in (001)-cut $\text{Pb}(\text{Mg}_{1/3}\text{Nb}_{2/3})_{1-x}\text{Ti}_x\text{O}_3$ single crystals

Authors: R. R. Chien, V. Hugo Schmidt, C.-S. Tu, and F. T. Wang

NOTICE: this is the author's version of a work that was accepted for publication in Journal of Crystal Growth. Changes resulting from the publishing process, such as peer review, editing, corrections, structural formatting, and other quality control mechanisms may not be reflected in this document. Changes may have been made to this work since it was submitted for publication. A definitive version was subsequently published in [Journal of Crystal Growth](#), VOL# 292, ISSUE# 2, (2006), DOI# [10.1016/j.jcrysgro.2006.04.046](https://doi.org/10.1016/j.jcrysgro.2006.04.046)

R.R. Chien, V.H. Schmidt, C.-S. Tu, and F.T. Wang, "Direct observation of ferroelectric domains and phases in (001)-cut  $\text{Pb}(\text{Mg}_{1/3}\text{Nb}_{2/3})_{1-x}\text{Ti}_x\text{O}_3$  single crystals," Journal of Crystal Growth 292, 395-398 (2006). doi: 10.1016/j.jcrysgro.2006.04.046.

# Direct observation of ferroelectric domains and phases in (001)-cut $\text{Pb}(\text{Mg}_{1/3}\text{Nb}_{2/3})_{1-x}\text{Ti}_x\text{O}_3$ single crystals under electric-field poling

R.R. Chien<sup>a,\*</sup>, V. Hugo Schmidt<sup>a</sup>, Chi-Shun Tu<sup>b</sup>, F.-T. Wang<sup>b</sup>

<sup>a</sup>Department of Physics, Montana State University, # 264 EPS Building, Bozeman, MT 59717, USA

<sup>b</sup>Graduate Institute of Applied Science and Engineering, Fu Jen University, Taipei 242, Taiwan, China

Available online 24 May 2006

---

## Abstract

Real-time direct observation of ferroelectric domains and phases under electric-field poling along [001] at room temperature in  $\text{Pb}(\text{Mg}_{1/3}\text{Nb}_{2/3})_{0.67}\text{Ti}_{0.33}\text{O}_3$  (PMNT33%) single crystal has been performed by polarizing microscopy. A hysteresis loop of polarization vs. electric field at room temperature was also measured for comparison. By using relations of crystallographic symmetry and optical extinction, polarizing microscopy reveals orientations of the domain polarizations and their corresponding phases. It also provides direct real-time observation of microcracking phenomena. It was found that the monoclinic phase domains play a crucial role in bridging higher symmetry (tetragonal and rhombohedral) phases while field-induced phase transitions take place.

© 2006 Elsevier B.V. All rights reserved.

PACS: 77.84.Dy; 77.80.Bh; 77.22.Ej; 77.80.Dj

Keywords: A1. Domain; A1. Electric-field poling; A1. Phase transition; B1. PMN-PT crystal

---

## 1. Introduction

Relaxor-based ferroelectrics  $\text{Pb}(\text{Mg}_{1/3}\text{Nb}_{2/3})_{1-x}\text{Ti}_x\text{O}_3$  (PMNT), which have a morphotropic phase boundary (MPB) between rhombohedral (R) and tetragonal (T) phases for  $0.26 \leq x \leq 0.36$  [1], have attracted much attention due to their high performance in piezoelectric-related applications. The ultrahigh piezoelectric response is attributed to polarization rotation induced by an external electric ( $E$ ) field between T and R phases through intermediate monoclinic (M) or orthorhombic (O) symmetries [2]. From our recent  $E$ -field-dependent domain study on (001)-cut PMNT24% and PMNT40% crystals at room temperature (RT), it was found that polarizations of the R (in PMNT24%) or T (PMNT40%) domains rotate toward the [001] tetragonal  $T_{001}$  phase through M distortions as  $E$  field increases along [001] [3,4]. To enhance piezoelectric performance, an  $E$ -field poling has usually been used on these materials before application. However, how poling affects phase stability and durability is still a critical

concern for long-term operation. In this report, we study  $E$ -field-dependent domains, phases, and microcracking phenomena at RT in a (001)-cut PMNT33% single crystal by polarizing microscopy and a hysteresis loop of polarization vs.  $E$  field. By using relations of crystallographic symmetry and optical extinction, polarizing microscopy can provide real-time direct observation of the polarization orientations in ferroelectric domains and their corresponding crystal phases under  $E$  field poling.

## 2. Experimental procedure

The lead magnesium niobate-lead titanate crystal PMNT33% was grown using a modified Bridgman method and was cut perpendicular to a  $\langle 001 \rangle$  direction by X-ray diffraction. Gold electrodes and transparent conductive films of indium tin oxide (ITO) were deposited, respectively, on sample surfaces by sputtering for measuring a hysteresis loop of polarization vs.  $E$  field and for  $E$ -field-dependent domain observation at RT. Before any measurement described below, the sample was annealed above 200 °C. For  $E$ -field-dependent domain observation with a DC field applied along [001], a Nikon E600POL polarizing

microscope was used with a  $0^\circ/90^\circ$  crossed polarizer/analyzer (P/A) pair. The experimental configuration can be found in Ref. [5]. The sample was polished to a thickness of  $65\mu\text{m}$ . The  $\langle 110 \rangle$  orientation of the sample edge was determined by X-ray diffraction and aligned with one of the crossed P/A: $0^\circ$  axes so that the extinction angles shown in all domain pictures are measured from  $\langle 110 \rangle$ . A hysteresis loop of polarization vs.  $E$  field (PEF) was measured at RT by using a Sawyer–Tower circuit at frequency 46 Hz.

### 3. Results and discussion

For interpreting polarizing microscopy domain observation among various phases, a review of principles of optical extinction for the (001)-cut crystal can be found in Ref. [6]. In this study, the extinction angles are measured with regard to  $\langle 110 \rangle$  as shown in Fig. 1. Thus, R domains represented by triangles with solid crosses in Fig. 1 have extinction at  $0^\circ$  ( $= 90^\circ$ ). T domains represented by squares with solid crosses have extinction at  $45^\circ$ . T domains with polarization  $P$  along the [001] axis represented by the solid black square in the center have extinction at every orientation of the crossed P/A pair and will be written as “ $T_{001}$ ” in the following discussion. The O domains represented by circles with solid crosses have extinctions at  $0^\circ$  ( $= 90^\circ$ ) or  $45^\circ$ , whereas R domains only give extinctions at  $0^\circ$ . Thus the (001) cut of Fig. 1 clearly distinguishes R from T phases by the  $45^\circ$  extinction angle

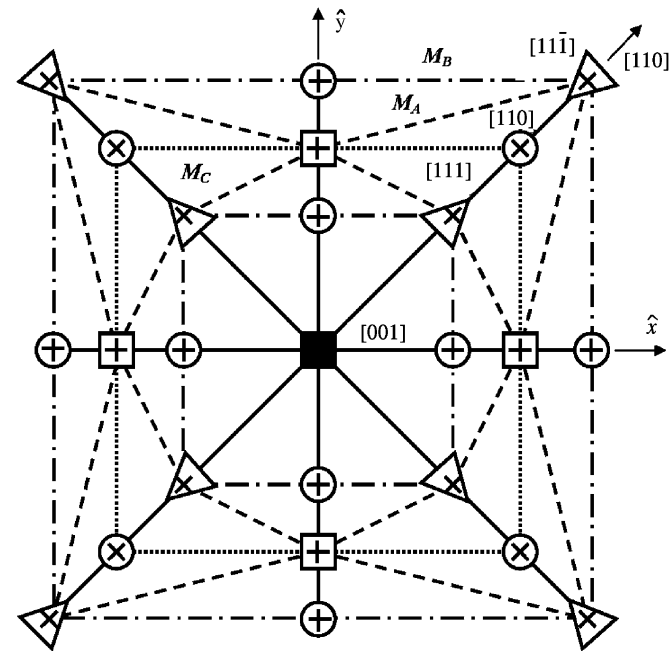


Fig. 1. Relation between the optical extinction orientations corresponding to the polarizations for various phases and domains projected on the (001) plane. Dashed, dash-dotted, and dotted lines represent  $M_A$ ,  $M_B$ , and  $M_C$  domains, respectively. The definition of  $M_A^-$ ,  $M_B^-$ , and  $M_C^-$  type monoclinic phases can be found in Ref. [7].

difference. Any extinction at angles other than  $0^\circ$  (or  $90^\circ$ ) and  $45^\circ$  must be from the M domains, or triclinic (Tri) domains. Note that all the phases except Tri phase have been reported in various PMNT crystals. Our large observed variation in extinction angle with  $E$  field indicates M domains whose polarization  $P$  can vary with  $E$  field through a large angle, whereas the direction of  $P$  is nearly fixed for a given R, T, or O domain as  $E$  field varies.

The  $E$ -field-dependent domain structures, as shown in Fig. 2, were taken at P/A: $45^\circ$  while a DC  $E$  field was applied along [001] at RT. At  $E = 0\text{ kV/cm}$  (Fig. 2(a)), the domain matrix mostly exhibits an extinction at  $0^\circ$  with respect to the  $\langle 110 \rangle$  direction as shown in the inset of Fig. 2(a). This indicates R phase. As the  $E$  field increases, the domain matrix does not essentially change until  $4.1\text{--}4.8\text{ kV/cm}$  as seen in Fig. 2(b). This is close to the

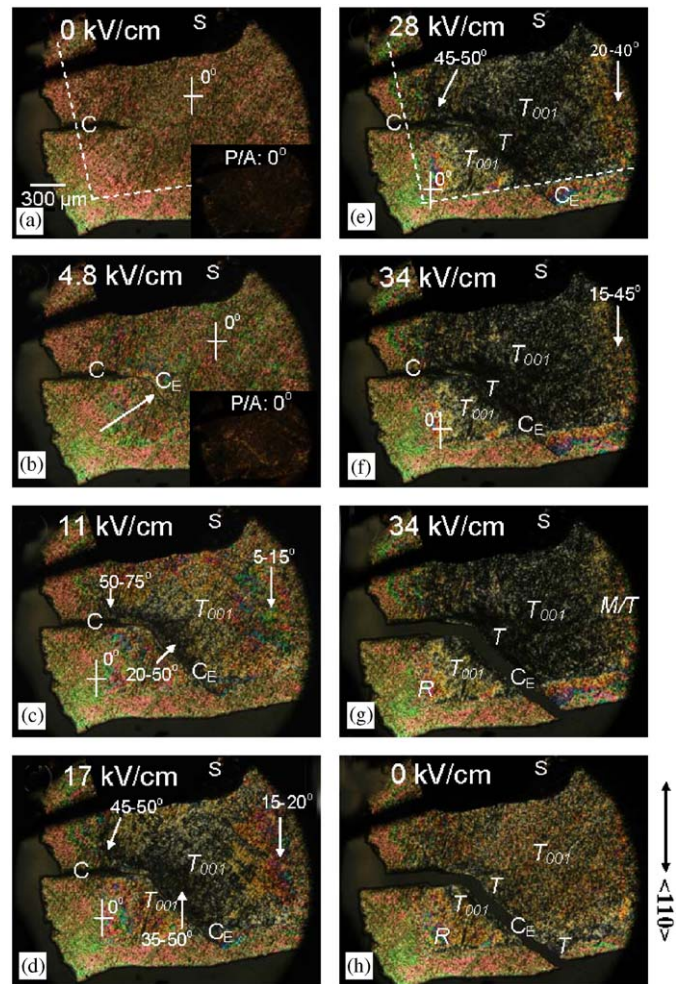


Fig. 2. Domain micrographs taken with P/A: $45^\circ$  (except the insets) at RT for  $E =$  (a)  $0\text{ kV/cm}$ , (b)  $4.8\text{ kV/cm}$ , (c)  $11\text{ kV/cm}$ , (d)  $17\text{ kV/cm}$ , (e)  $28\text{ kV/cm}$ , (f)  $34\text{ kV/cm}$ , (g)  $34\text{ kV/cm}$  (the crystal breaks), and (h) right after the  $E$  field was removed. The area in black indicated by “S” is the silver paste and the wire. “C” and “ $C_E$ ” are the cracks caused by polishing and poling, respectively. The dashed line shows the ITO film’s boundary. The angles and locations of domain extinctions are indicated by the degrees and arrows. The tetragonal [001] phase domains induced by the  $E$  field are indicated by  $T_{001}$ .

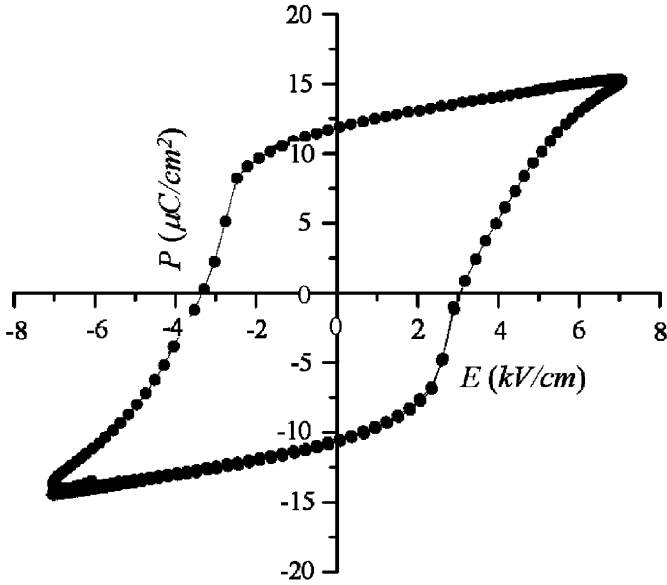


Fig. 3. Hysteresis loop of polarization vs.  $E$  field obtained at RT.

coercive field  $E_C \sim 3$  kV/cm, as shown in Fig. 3. The domain matrix mostly still retains the R phase [inset of Fig. 2(b)], but  $T_{001}$  and M/T phases were induced near the cracking area and exhibit extinctions at all P/A angles and  $\sim 15\text{--}65^\circ$ , respectively. M/T represents the coexistence of M and T phase domains with more M phase than T phase. As the field increases to 11 kV/cm (Fig. 2(c)), the  $E$ -field-induced  $T_{001}$  phase domain significantly expands as crossed stripes along  $[100]$  and  $[010]$  from the cracking area. Some of the other R phase domains have also transformed to M and T phase domains with various nonzero-degree extinction angles, such as  $5\text{--}15^\circ$ ,  $20\text{--}50^\circ$ , and  $50\text{--}75^\circ$ . But the lower left-hand corner of the domain matrix still remains in the R phase, as indicated with extinction angle  $0^\circ$ . With the  $E$  field increasing to 34 kV/cm, this  $E$ -field-induced transition is continuously evidenced by the expansion of the  $T_{001}$  phase domain as shown in Figs. 2(d)–(f). At  $E = 34$  kV/cm, most of the domain matrix becomes macroscopic  $T_{001}$  phase domain except for some small R, T, and M phase domains with extinction angles of  $0^\circ$ ,  $45^\circ$ , and  $\sim 15\text{--}45^\circ$  as illustrated in Fig. 2(f). It is interesting that T phase domains usually appear near the cracks. In addition, a few domains exhibiting no extinction at any P/A angle are embedded in the  $T_{001}$  phase domain matrix perhaps due to local strained regions caused by underlying M distortions with several different orientations.

As indicated by the arrow and “ $C_E$ ” in Fig. 2(b), the microcracking caused by the DC  $E$ -field poling process starts to develop at  $\sim 4.8$  kV/cm along  $[100]$  (or  $[010]$ ) from the pre-existing crack “C” caused by the polishing process. The crack is enlarged by the increasing field strength as shown in Figs. 2(c)–(f). As the field increases to 34 kV/cm (Fig. 2(g)), the crack reaches the edge of the sample and the crystal breaks. The crystal still maintains the same R, T,  $T_{001}$ , and M phase domains as before it

breaks (Fig. 2(f)). After the field is removed (Fig. 2(h)), the polarizing microscope picture becomes brighter than for  $E = 34$  kV/cm (Fig. 2(g)), but the crystal does not return to an R phase as seen originally at zero field (Fig. 2(a)). Instead, the speckled appearance of the picture implies that R,  $T_{001}$ , T, and M phase microdomains coexist with numerous microdomains that have no extinction at any P/A angle, which perhaps is caused by the stress exerted by local polar microdomains of M phases with various orientations. In our recent study, a (001)-cut PMNT40% single crystal becomes entirely  $T_{001}$  phase monodomain near 33 kV/cm and its microcracking phenomenon starts near 12.5 kV/cm and develops along  $[010]$  [4]. However, a (001)-cut rhombohedral PMNT24% single crystal cannot reach a  $T_{001}$  phase monodomain and no microcracking was found under a higher  $E$  field (44 kV/cm) applied along  $[001]$  at RT [3].

What is the transition mechanism while  $T_{001}$  phase domains are induced by a DC  $E$  field applied along  $[001]$  in PMNT crystals? In the (001)-cut PMNT24% crystal, the  $T_{001}$  phase domains are induced near 4 kV/cm by polarization rotation of R to  $T_{001}$  phase through M distortions as  $E$  field increases along  $[001]$  at RT [3]. In the (001)-cut PMNT40% crystal, the  $T_{001}$  phase domains are induced near 11 kV/cm at RT by the process  $T \rightarrow M \rightarrow T_{001}$ , and this  $T_{001}$  phase expands through the whole crystal by the process as the  $E$  field increases further [4]. Similarly, in this (001)-cut PMNT33% crystal, the  $T_{001}$  phase domains are induced near 4.1 kV/cm and expand significantly at 11 kV/cm at RT by the processes  $R \rightarrow T_{001}$ ,  $R \rightarrow M \rightarrow T_{001}$ ,  $R \rightarrow T \rightarrow T_{001}$ , and  $R \rightarrow M \rightarrow T \rightarrow T_{001}$ . These  $T_{001}$  phase domains expand through the whole crystal by these processes with increasing  $E$  field.

#### 4. Conclusions

Polarizing microscopy is a powerful tool to visualize phase transformation and domain orientation. It also provides a direct real-time observation under application of a DC  $E$  field of the microcracking, which has been an obstacle for applications of medical imaging, telecommunication, and ultrasonic devices based on these crystals. Microcracking was found in the tetragonal crystal [4], but no microcracking was found in the rhombohedral crystal under a high electric field (44 kV/cm) [3]. Microcracking can also be triggered by a pre-existing crack in the crystal as evidenced in this study. In addition, we have found that microcracks are inclined to develop along  $[100]$  (or  $[010]$ ), which is the growth direction of the  $T_{001}$  phase domain, while the  $T_{001}$  domain is induced by a DC  $E$  field applied along  $[001]$ . With the maximum strength of  $E$  field, a single domain with the orientation along the poling  $E$  field was not always obtained in every crystal as expected, such as the (001)-cut PMNT24% [3]. Importantly, it was found that the M phase plays an essential role in bridging higher symmetries while  $E$ -field-induced phase transitions are taking place in all three crystals with the same cut but

different titanium content (PMNT $x$ %,  $x = 24, 33,$  and  $40$ ) across the MPB range.

### Acknowledgment

This work was supported by DoD EPSCoR Grant no. N00014-02-1-0657 and NSC Grant no. 94-2112-M-030-004.

### References

[1] T.R. Shrout, Z.P. Chang, N. Kim, S. Markgraf, *Ferroelectrics Lett.* 12 (1990) 63.

[2] H. Fu, R.E. Cohen, *Nature* 403 (2000) 281.

[3] R.R. Chien, V.H. Schmidt, C.-S. Tu, L.-W. Hung, H. Luo, *Phys. Rev. B* 69 (2004) 172101.

[4] R.R. Chien, V.H. Schmidt, L.-W. Hung, C.-S. Tu, *J. Appl. Phys.* 97 (2005) 114112.

[5] C.-S. Tu, V.H. Schmidt, I.-C. Shih, R. Chien, *Phys. Rev. B* 67 (2003) 020102.

[6] V.H. Schmidt, R. Chien, I.-C. Shih, C.-S. Tu, *AIP Conf. Proc.* 677 (2003) 160.

[7] D. Vanderbilt, M.H. Cohen, *Phys. Rev. B* 63 (2001) 094108.